AD-A190 038 FUNDAMENTAL STUDIES OF THE MECHANICAL BEHAVIOR OF MICROELECRRONIC THIN FI (U) STANFORD UNIV CA DEPT OF MATERIALS SCIENCE AND ENGINEERING W D NIX DEC 87 1/1

UNCLASSIFIED AFOSR-TR-88-0161 AFOSR-86-0051 F/G 20/12 NL

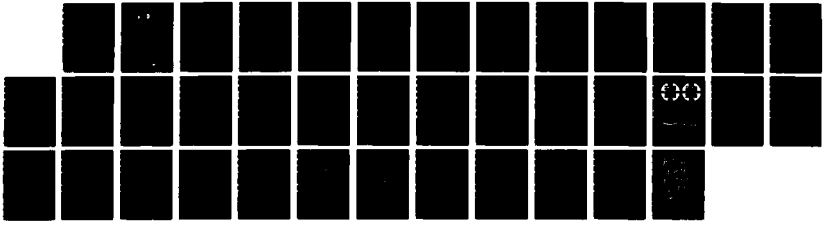

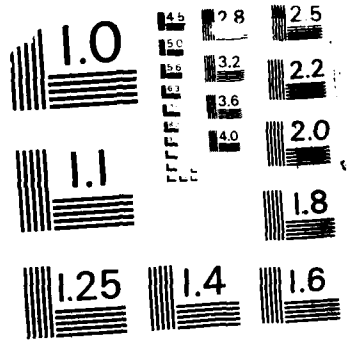

DTIC FILE COPY

FEB 1988

SECURITY CLASSIFICATION OF THIS PAGE

REPORT DOCUMENTATION PAGE

Form Approved OMB No. 0704-0188

AD-A190 038

DTIC ELECTE FEB 29 1988 D

1b. RESTRICTIVE MARKINGS	
2b. DECLASSIFICATION/DOWNGRADING SCHEDULE	3. DISTRIBUTION/AVAILABILITY OF REPORT: Approved for public release, distribution unlimited
4. PERFORMING ORGANIZATION REPORT NUMBER(S)	5. MONITORING ORGANIZATION REPORT NUMBER(S): AFOSR-TR- 88-0161
6a. NAME OF PERFORMING ORGANIZATION: Stanford University	6b. OFFICE SYMBOL (If applicable):
6c. ADDRESS (City, State, and ZIP Code): Stanford CA 94305	7a. NAME OF MONITORING ORGANIZATION: AFOSR/NE
	7b. ADDRESS (City, State, and ZIP Code): Bldg 410, Bolling AFB, DC 20332-6448
8a. NAME OF FUNDING/SPONSORING ORGANIZATION: SAME AS 7 a	8b. OFFICE SYMBOL (If applicable):
	9. PROCUREMENT INSTRUMENT IDENTIFICATION NUMBER: AFOSR-86-0051
8c. ADDRESS (City, State, and ZIP Code): SAME AS 7b	10. SOURCE OF FUNDING NUMBERS

PROGRAM ELEMENT NO.	PROJECT NO.	TASK NO	WORK UNIT ACCESSION NO.
61102F	2306	A1	

11. TITLE (Include Security Classification)
FUNDAMENTAL STUDIES OF THE MECHANICAL BEHAVIOR OF MICROELECTRONIC THIN FILM MATERIALS

12. PERSONAL AUTHOR(S)
Professor William D Nix

13a. TYPE OF REPORT	13b. TIME COVERED	14. DATE OF REPORT (Year, Month, Day)	15. PAGE COUNT
Annual REport	FROM 01/11/86 TO 31/10/87	Dec 87	

16. SUPPLEMENTARY NOTATION

17. COSATI CODES			18. SUBJECT TERMS (Continue on reverse if necessary and identify by block number)
FIELD	GROUP	SUB-GROUP	

19. ABSTRACT (Continue on reverse if necessary and identify by block number)

A fundamental program of research on the mechanical properties of microelectronic thin film materials is underway at Stanford University. The work is being supported under AFOSR Grant No. 86-0051. In this interim Scientific Report, some of the progress made during the second year of the program is reviewed. We have made rapid progress since starting this development of new experimental techniques for measuring mechanical properties of thin films. That work led to several publications and to an equal number of invited oratl presentations, both of which are listed at the end of this report. Now much of our work involves the use of these techniques to study mechanical properties of thin film materials of interest in microelectronics.

20. DISTRIBUTION/AVAILABILITY OF ABSTRACT	21. ABSTRACT SECURITY CLASSIFICATION
☐ UNCLASSIFIED/UNLIMITED ☐ SAME AS RPT. ☐ DTIC USERS	UNCLASSIFIED
22a NAME OF RESPONSIBLE INDIVIDUAL: ROSENSTEIN	22b. TELEPHONE (Include Area Code): (202) 767-4933 / 22c. OFFICE SYMBOL: NE

DD Form 1473, JUN 86 — Previous editions are obsolete. — SECURITY CLASSIFICATION OF THIS PAGE

Interim Scientific Report
(For the Period 1 November 1986 to 31 October 1987)
AFOSR GRANT NO. 86-0051

FUNDAMENTAL STUDIES OF THE MECHANICAL BEHAVIOR OF MICROELECTRONIC THIN FILM MATERIALS

Submitted to:

Department of the Air Force
Directorate of Electronic and Material Sciences
Air Force Office of Scientific Research
Bolling Air Force Base, Building 410
Washington, D.C. 20332

Attention: Dr. Alan H. Rosenstein

Submitted by:

Professor William D. Nix, Principal Investigator
Department of Materials Science and Engineering
Stanford University, Stanford California 94305

December 1987

This research was supported by the Air Force of Scientific Research (AFOSC) under Grant No. AFOSR-86-0051. Approved for public release; distribution unlimited.

Table of Contents

I. Summary

A fundamental program of research on the mechanical properties of microelectronic thin film materials is underway at Stanford University. The work is being supported under AFOSR Grant No. 86-0051. In this Interim Scientific Report, some of the progress made during the second year of the program is reviewed. We have made rapid progress since starting this research program just two years ago. Much of our early work involved the development of new experimental techniques for measuring mechanical properties of thin films. That work led to several publications and to an equal number of invited oral presentations, both of which are listed at the end of this report. Now much of our work involves the use of these techniques to study mechanical properties of thin film materials of interest in microelectronics.

The primary motivation of this work is to understand the mechanical properties of microelectronic thin film materials. Although these materials are not structural materials as such, they are, nevertheless, expected to withstand very high stresses, both during manufacturing and in service. As a consequence, the mechanical properties of these materials are almost as important as their electronic properties for successful device applications. Because these materials often exist only as thin films bonded to substrates, it is necessary to study their mechanical properties in that state. For this reason most of our work to date has involved the development and use of submicron indentation and wafer curvature techniques for studying the mechanical properties of thin films on substrates.

The mechanical behavior or response of microelectronic thin films is caused by the very large stresses that can exist in these materials. For this reason it is important to have a clear understanding of how these stresses originate. Thermal and epitaxial stresses are quite well understood and in cases where these processes dominate it is relatively easy to predict the resulting stresses. Often, however, the stresses that act in thin film structures are the result of non-equilibrium growth processes. During the past year we have made a study of the physical processes by which "intrinsic" (or growth)

stresses are generated in thin film structures. That work will appear as a special review paper (to be published by CRC) and is not summarized here.

The central equation in the study of stresses and mechanical properties of thin films on substrates involves the relationship between the stress in the film and the corresponding curvature of the substrate. The equation that is commonly used to interpret experiments is based on several well known approximations that are considered to hold for the typical case of a thin film on a relatively thick substrate. Other approximations that are implicit in the use of the standard formula have not been studied in detail. During the past year we have studied the effects of gravity and support geometry on the film stress-curvature relationship. We find that the way the substrate is supported can have significant effects on the curvature because the pull of gravity causes the substrate to bend in a measurable way. This analysis shows why it is important to have a reproducible way to support the substrate when the film stress is being measured. We have also studied the effects of substrate shape, elastic anisotropy in the substrate and thermal gradients in the substrate on the stress-curvature relationship. These effects appear to be much less significant than those associated with gravity

An experiment has been designed to study the basic mechanisms of crack formation in interconnect metals. We have proposed to use the wafer curvature apparatus to monitor the cracking of aluminum lines under a rigid passivation. A pattern or mask has been made for this purpose and test samples are now being made. We hope to be able to study the kinetics of cracking as a function of stress and temperature using this technique. The motivation for this work and progress made during the past year are described in the report.

One of the basic mechanisms of deformation of thin films involves the interaction of dislocations with interfaces. In the first year of this program we studied the long range interactions of screw dislocations with the many interfaces that are present in thin film structures. During the past year we have started to extend this analysis to the case of short range interactions, where a given dislocation comes into intimate contact with an interface. Progress on this theoretical problem is described in the report.

II. Research Report

A. Some Issues Concerning Curvature of a Plate Relevant To Thin-Film Stress Analysis

(F. von Preissig)

1. Introduction

Thin solid films of many kinds, deposited or grown onto substrates, are used in today's microelectronic devices. Mechanical stresses in these films arise from various causes, including thermal expansion differences between film and substrate materials, the chemical state of the as-deposited material, and chemical or structural changes occurring in the films upon processing after deposition. These stresses can lead to cracking or delamination of the films and can induce dislocation formation in the substrate. The study of film stress is also of interest as a probe of the physico-chemical nature of the film material.

In order to experimentally determine mechanical stresses in thin films on substrates, it is common practice to use the formula

$$C = \frac{1}{R} = \frac{6(1-\nu)\sigma d}{Et^2}, \qquad (1)$$

where

C = curvature of substrate; R = radius of curvature
E = Young's modulus of substrate
ν = Poisson's ratio of substrate
d = film thickness
t = substrate thickness
σ = In-plane film stress.

Eqn. (1) has been derived [1, 2, 3a] for the following case: The substrate is a plate that is thin, elastically isotropic, and (when bare) flat. The single film has uniform thickness, much less than t, and a uniform, isotropic plane stress. The temperature is uniform. The maximum displacement due to bending is less than about $t/2$. The composite plate (substrate plus film) is mechanically free.

Hence, by measuring the radius of curvature of a film-substrate composite (e.g., by an optical lever technique), film stress can, in principle, be calculated.

In practice, however, conditions arise that completely invalidate eqn. (1), require it to be modified somewhat, or simply call its accuracy into question, pending further investigation. For example, if the substrate is initially not quite flat, or if it is subjected to small, reproducible deformations other than that caused by the film stress, eqn. (1) may apply only after the non-film-stress effects are subtracted out, e.g., by making a reference measurement of the bare-substrate surface profile [4]. Also, thick-film and multiple-film cases are covered by extensions to eqn. (1) that have already been derived [5, 6]. In this report, I examine (mostly theoretically) some of the effects of gravity, substrate shape, substrate crystallinity, and temperature gradients on substrate curvature.

2. Geometric Conventions and Basic Formulas

Geometric conventions for the composite plate as defined in Fig. 1 are adopted. Radial symmetry about the *z*-axis is assumed.

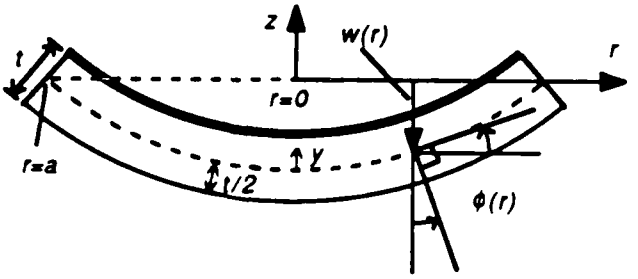

Figure 1. Geometry (exaggerated) of a bent, circular plate with film. a = radius, r = radial position, w = displacement, y = level, and ϕ = slope.

The slope is given by

$$\phi(r) = -\frac{dw}{dr} . \qquad (2)$$

For small deflections, the local curvature is

$$C(r) = \frac{d\phi}{dr} = -\frac{d^2 w}{dr^2} \tag{3}$$

(shown positive in Fig. 1).
If, in addition, C is constant over r, then

$$\phi(r) = \int_0^r C(r)dr = Cr \tag{4}$$

and

$$w_{max} = \frac{1}{2}aC . \tag{5}$$

The effect of the film on the composite-plate thickness and rigidity is negligible since $d << t$ will always be assumed. The film stress is positive when tensile. Bending moments per unit length, M, are positive if they tend to cause positive curvature in their plane of action.

The substrate, unless otherwise noted, is considered to be a *thin plate* subjected to *small deformations,* as defined below (from [7a]):

> In the theory of thin plates, it is customary to make the following assumptions: 1) The plate is initially flat. 2) The material is elastic, homogeneous, and isotropic. 3) Thickness is small compared to area dimensions. 4) Slope of the deflection surface is small compared to unity. 5) Deformation is such that straight lines initially normal to the middle surface remain straight and normal to that surface. (Vertical shear strains are neglected.) 6) Strains in the middle surface, arising from the deflection, are neglected compared to strains due to bending. 7) Deflection of the plate occurs by virtue of displacement of points in the mid-surface normal to its initial plane. 8) Direct stress normal to the middle surface is neglected. 9) Near edges and boundaries of loaded areas, stress resultants rather than detailed stress patterns are considered.

The flexural rigidity of the plate is defined as

$$H = \frac{Et^3}{12(1-\nu^2)} . \tag{6}$$

The biaxial modulus is

$$\beta = \frac{E}{1-\nu} . \tag{7}$$

3. Effect of Gravity

In real situations, the sample is not free, but is typically supported from below and subjected to the downward pull of gravity. The manner in which this uniform force affects the curvature depends on the position of the support points. If the support points are reproducible, as they are in a tripod arrangement of pins, then the effect of gravity on a given wafer (sample) is constant and can be subtracted out by making a bare-wafer measurement. If, however, the wafer sits on a flat surface (sometimes a tripod support is impractical), the wafer's support points will depend on the wafer's warp. In this case, it is desirable to have an estimate of the maximum change in curvature associated with a change in support points.

Take as two extremes a round plate 1) simply supported from below all around its perimeter and 2) supported only at its center. With q defined as the uniform downward force per area, the displacement of the plate for the edge-supported case is given by [7b]

$$w_{edge} = \frac{qa^2}{64H}\left(1-\frac{r^2}{a^2}\right)\left(\frac{5+\nu}{1+\nu}-\frac{r^2}{a^2}\right). \qquad (8)$$

The displacement for the center-supported case can be calculated by superimposing the solutions to two different loading situations, as shown in Figure 2.

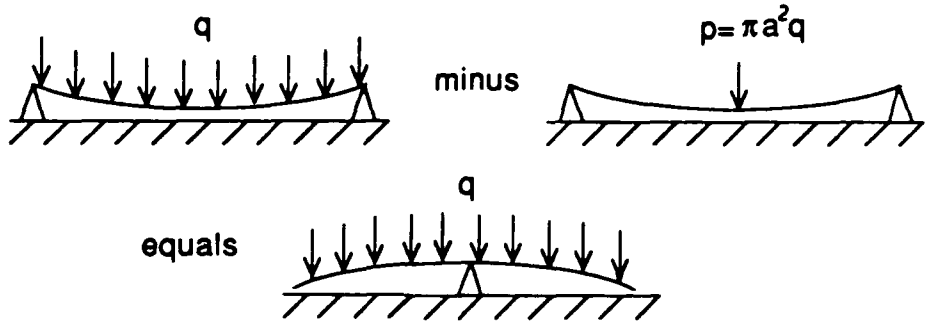

Figure 2. Demonstration of the way in which the center-supported elastic plate-bending case is derived from the superposition of two other cases.

The result is

$$w_{center} =$$

$$w_{edge} - \frac{qa^4}{16H}\left[2\frac{r^2}{a^2}\ln\left(\frac{r}{a}\right) + \frac{3+\nu}{1+\nu}\left(1-\frac{r^2}{a^2}\right)\right]. \qquad (9)$$

The difference between the edge and center cases is

$$\Delta w = w_{edge} - w_{center} =$$

$$\frac{qa^4}{16H}\left[2\frac{r^2}{a^2}\ln\left(\frac{r}{a}\right) + \frac{3+\nu}{1+\nu}\left(1-\frac{r^2}{a^2}\right)\right]. \qquad (10)$$

The corresponding local shape and curvature, after substituting $q = Dt$, where D is substrate weight density, are

$$\Delta\phi(r) = -\frac{d(\Delta w)}{dr} =$$

$$\frac{Dta^2 r}{4H}\left[\frac{1}{1+\nu} - \ln\left(\frac{r}{a}\right)\right] =$$

$$\frac{3Da^2 r}{\beta t^2}\left[1-(1+\nu)\ln\left(\frac{r}{a}\right)\right], \qquad (11)$$

$$\Delta C(r) = -\frac{d^2(\Delta w)}{dr^2} =$$

$$-\frac{Dta^2}{4H}\left[\frac{\nu}{1+\nu} + \ln\left(\frac{r}{a}\right)\right] =$$

$$-\frac{3Da^2}{\beta t^2}\left[\nu + (1+\nu)\ln\left(\frac{r}{a}\right)\right]. \qquad (12)$$

(The mathematical singularity at $r = 0$ makes (12) physically unrealistic very near the center.)

The average of ΔC from $r = 0$ to $r = r$ on the wafer is

$$\overline{\Delta C}(r) = \frac{1}{r}\int_0^r \Delta C(r)dr =$$

$$\frac{1}{r}[\Delta\phi(r) - \Delta\phi(r \to 0)] =$$

$$\frac{3Da^2}{\beta t^2}\left[1-(1+\nu)\ln\left(\frac{r}{a}\right)\right]. \qquad (13a)$$

For the whole radius (or diameter, due to symmetry), this average reduces to

$$\overline{\Delta C}(a) = \left(\frac{3Da^2}{\beta t^2}\right). \qquad (13b)$$

Typically, however, what curvature measurement techniques (such as ours) actually record is an average curvature that is calculated as the slope of a linear regression best-fit line for a series of measured slope *vs.* diametral-position data points. If the curvature is not constant (and there are more than two data points), then the measured curvature, C_M, will not in general equal the true average of C over r, $\overline{C}(r)$. The theoretical value of C_M can be derived from $C(r)$. Taking $C(r)$ to be the gravity effect ($\Delta C(r)$) given by eqn. (12) and using ten slope measurements equally spaced on a wafer diameter for C_M, one can calculate that

$$C_M / \overline{\Delta C}(a) = 1.237 + 0.237\nu, \qquad (14)$$

which equals 1.27 for a quartz substrate ($\nu = .16$) and has a maximum possible value of 1.36 (when $\nu = .5$). The ratio $C_M/\overline{\Delta C}(r)$ is closer to 1 for measurements spanning less than the full diameter (i.e. $r < a$). We will subsequently to refer to the gravity effect in terms of $\overline{\Delta C}(a)$, keeping in mind that C_M is comparable to $\overline{\Delta C}(a)$.

In determining the film stress, we may view the maximum gravity effect as a component of the experimental uncertainty. With C_o defined as the curvature due to film stress alone, as given by eqn. (1), then

$$\frac{\overline{\Delta C}(a)}{C_o} = \frac{Da^2}{2\sigma d}. \qquad (15)$$

Note that this relative variation is independent of substrate moduli and thickness, but is a strong function of wafer size. To reduce the relative gravity effect, one can simply use smaller substrates.

Take the example of a silicon (D = 2.33 g/cm^3 x 980.7 dyne/gram-force) substrate (say (111)-oriented, which is elastically isotropic in-plane) with a typical film having σ = 200 MPa = 2x10^9 dyne/cm^2 and d = .5μ = 5x10^{-5} cm. If the substrate is a 100-mm wafer (a = 5 cm), then eqn. (15) gives a relative uncertainty of 29%. But a = 1 cm yields a very tolerable uncertainty of 1.1%. For a substrate of quartz (D = 2.2 g/cm^3, β = 8.6X10^{11} dyne/cm^2, ν = .16 [8]), the relative gravity effect is slightly less than it is for silicon, although the absolute effect is larger.

Experimental confirmation of the gravity effect theory is shown in Figure 3. In this case, what is plotted is -dw/dx *vs.* x, where x is the diametral position, with the center of the wafer being at x = 0, and -dw/dx is the slope of the wafer surface. The appropriate theoretical equation, a modification of eqn. (11), is

$$-\frac{d(\Delta w)}{dx}(x) = \frac{3Da^2}{\beta t^2}\left[1-(1+\nu)\ln\left|\frac{x}{a}\right|\right]. \qquad (16)$$

Experimentally, slope *vs.* position data for a round quartz substrate were obtained using a laser reflection technique. The slopes that were measured while the substrate was supported at its center by a 2-mm Si chip were subtracted (for each position) from the slopes measured when the substrate was supported around its edge by a foam ring. The resulting experimental values fit the theoretical curve quite well.

It should be noted, however, that plate deflection is very sensitive to the boundary conditions, and that in this case, a uniform, simple edge support was hard to achieve. This difficulty resulted in some measurements varying as much as 30% from those shown. In fact, in an experiment in which the edge of the substrate was intentionally supported at only two points, on the line of measurement, the edge-minus-center measured curvature was 2.17x10^{-2} m^{-1}, or 2.2 times what it was with the uniform edge support. Hence the "two extremes" of support for which the equations of this section have been derived do not represent the absolute extremes of gravitational bending of an isotropic, round substrate (to say nothing of a

crystalline or rectangular one). Nevertheless, our analysis explains the general magnitude of the gravity effect and shows how this effect can be altered by using different substrate materials and sizes. Such knowledge can be useful in the design of experiments and the interpretation of their results.

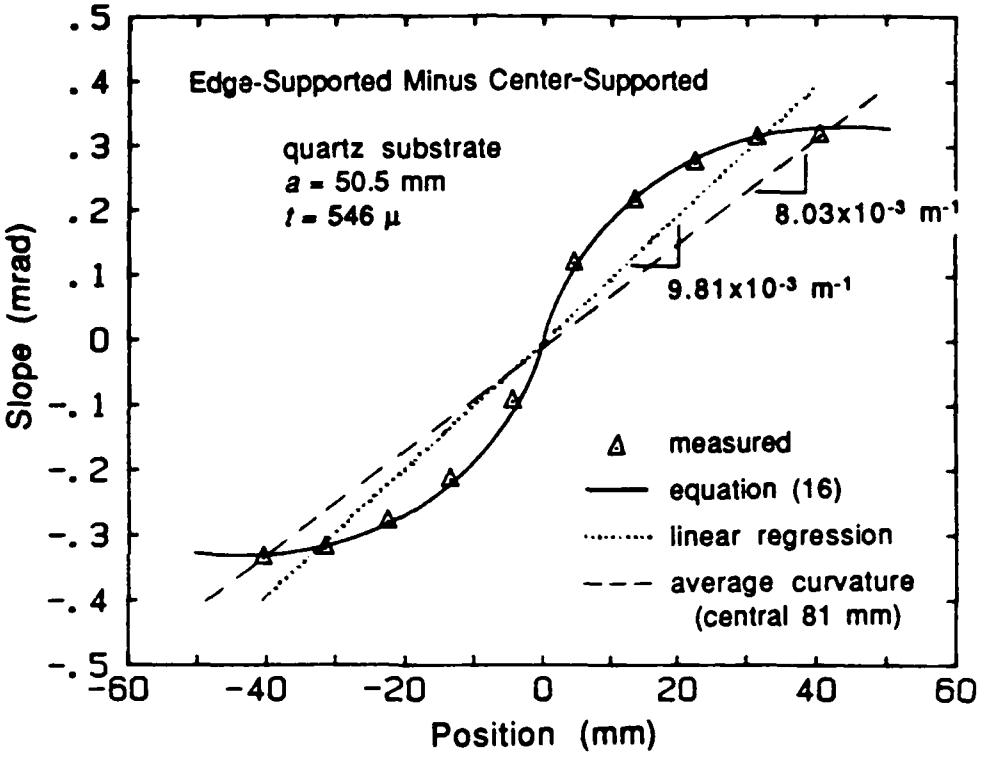

Figure 3. Experimental confirmation of gravity effect on quartz substrate.

4. Effect of Shape

Most researchers doing experiments that employ eqn. (1) nowadays use round substrates, usually silicon wafers. But the substrate does not need to be round for (1) to hold, as the simple derivation presented here will demonstrate.

Timoshenko [9] has shown that a rectangular plate with a uniform bending moment per unit length M applied at its edges will deform into a spherical cap having a curvature

$$C = \frac{M}{H(1+\nu)} \qquad (17)$$

and an internal bending moment isotropically and uniformly equal to M. Hence, a plate of *any* shape will deform in accordance with eqn. (17) if M is applied to its edges, since the same boundary conditions are applied to any internal section of the rectangular plate.

In a "strength of materials" analysis of the effect that a thin, stressed film has on a substrate, a force and bending moment acting on the perimeter of the substrate are found that make the resultant force and moment at the edge of the film plus substrate equal zero, as illustrated in Fig. 4. The bending moment per unit length is approximately

$$M = \frac{1}{2} t\sigma d. \qquad (18)$$

(The net edge force has a negligible effect on substrate curvature.) Substitution of (18) into (17) yields (1). Thus, under conditions in which eqn. (1) holds for a round substrate, it also holds for a substrate plate of any other shape.

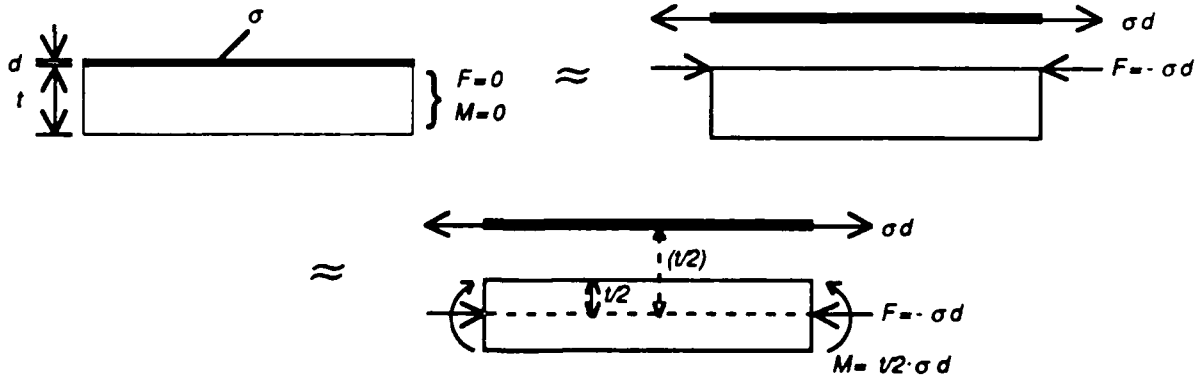

Figure 4. Model of how a thin film exerts the approximate equivalent of a bending moment per unit length M on the edge of a substrate.

However, the substrate must not be narrower than about $4t$, or it will cease to bend like a plate [3b]. If the width is about equal to t or smaller, beam theory applies and $Et^3/12$ replaces H (e.g., in (18)).

5. Effect of Crystallinity

At the outset, I stated that eqn. (1) was derived based on the assumption that the substrate is elastically isotropic. Yet single-crystal silicon is often employed as the substrate material. In this section, I explain why the substrate crystallinity does not necessarily invalidate (1). My approach is to verify that (1) is entirely consistent with elastic theory for a cubic crystal such as silicon.

When a substrate plate is bent to a uniform curvature (as required by (1)), it has an in-plane strain distribution given by

$$e_{plane}(y) = -Cy, \tag{19}$$

where y is the distance measured from the plate's middle surface toward its upper (or film-covered) surface. If this plate is made of an isotropic material, the in-plane stress is related to the in-plane strain by

$$\sigma_{plane} = \beta e_{plane}, \tag{20}$$

where σ_{plane} and e_{plane} are biaxial (planar-isotropic). Combining (19) and (20), we obtain

$$\sigma_{plane}(y) = -C\beta y, \tag{21}$$

and then

$$M = -\int_{-\frac{t}{2}}^{\frac{t}{2}} \sigma(y)\, y\, dy = \frac{C\beta t^3}{12}. \tag{22}$$

Substituting M induced by the film, given by eqn. (18), yields equation (1).

If the substrate is *not* made of an isotropic material, the preceding analysis proves that (1) is equally valid as long as (20), a constitutive equation, holds. The stress state satisfies the equilibrium equations of continuum mechanics, the strain state satisfies continuity requirements, and the physical conditions satisfy all boundary requirements, just as they do when the material is isotropic.

It is known [10] that $E/(1-\nu)$ (β) is invariant for directions within {100} and {111} planes of cubic crystals, and hence isotropic in-plane in (100)- and (111)-oriented silicon wafers. For {111} planes, E and ν are individually invariant, and as a result, these planes are truly elastically isotropic. But for {100} planes, E and ν are not invariant. Hence, the question is whether a planar-isotropic β is sufficient to make eqn. (20) true.

Hooke's Law for elastic anisotropic media, in reduced notation, is

$$e_i = S_{ij}\sigma_j, \tag{23a}$$

Where $i, j = 1, 2, \ldots 6$ represent "tensile" or "shear" together with directionality, and the S_{ij} are the standard elastic compliances of the crystal. If the orthogonal coordinate axes are not specified as coincident with the <100> crystal directions, the equation is rewritten as

$$e'_i = S'_{ij}\sigma'_j. \tag{23b}$$

Although for a cubic crystal, many of the S_{ij} are zero, this is not the case, in general, for the S'_{ij}.

Now take the x and y axes of the coordinate system to be at arbitrary (but perpendicular) positions within the plane of the crystal substrate. In the biaxial stress state proposed above, there are two principal tensile stress components, $\sigma'_1 = \sigma'_2$, all other σ'_j being zero. For this case, (23b) reduces to

$$e'_1 = (S'_{11} + S'_{12})\sigma'_1 \tag{24}$$

for $i = 1$. Here e'_1 is the tensile strain for an arbitrary direction within the substrate plane. Note that

$$S'_{11} + S'_{12} = S'_{11}\left(1 + \frac{S'_{12}}{S'_{11}}\right) = \frac{1}{E'_{11}}(1 - \nu'_{12}) = \frac{1}{\beta'_{12}}, \tag{25}$$

and hence

$$\sigma'_1 = \beta'_{12} e'_1. \qquad (26)$$

Thus, if β'_{12}, i.e., β for arbitrary in-plane directions, is isotropic, as it is for (100) and (111) silicon, it relates a biaxial stress state to a biaxial strain state without contradiction. Equation (20) does hold, so eqn. (1) is valid for (100) and (111) silicon substrates.

It should be mentioned that eqns. (24) and (26) do not hold in situations where the stress and strain states are not biaxial. Nonspherical bending due to gravity is one such case. Thus, a (100) silicon wafer will not sag as if it were isotropic; its slope distribution is not expected to be radially symmetric. However, since the gravity-effect slope and average curvature equations, (11) and (12), depend strongly on β, compared to an additional dependence on ν, asymmetry should be slight and use of an average value of ν should suffice for most purposes.

6. Effect of Thermal Gradient

In some experiments, a film on a substrate is heated while the curvature is being measured in order to determine the effect of temperature changes and annealing on film stress. Thermal gradients may exist in the substrate, and their effect on the curvature must be considered.

We will examine the case where the substrate has a temperature that varies linearly from T at the top surface to $T + \Delta T$ at the bottom surface. This vertical thermal gradient contributes directly to curvature, since the thermal strain varies linearly with level. The thermally-induced curvature, which is uniform over r, is [3c]

$$C_{therm} = \frac{\alpha \Delta T}{t}, \qquad (27)$$

where α is the thermal expansion coefficient of the substrate. This equation can easily be derived using eqn. (19).

In the following examples, we will use the material parameters given in Table 1 [11, 12].

Table 1

	Thermal Exp. Coef.†		Thermal Conductivity‡	
	α, 25° C	α, 700° C	k, 300° C	k, 700° C
Silicon	2.6	4.4	136	32
Fused Quartz	.50	.39	1.7	2.7

†(10^{-6} °C^{-1})
‡(W/m°C)

Suppose we wish to know what ΔT would cause a C_{therm} of $1x10^{-3}$ m^{-1}, which is a small but significant curvature change, in a .5 mm-thick substrate. From eqn. (27), $\Delta T = Ct/\alpha$ =

for silicon: .19 C° at 25° C , .32 C° at 700° C;

for quartz: 1.0 C° at 25° C , .78 C° at 700° C.

Let us calculate how much power must pass vertically through a round 100-mm wafer to cause the above effects.

$$\text{Heat flow rate} = kA\frac{\Delta T}{\Delta x}; \qquad (28)$$

$A = \pi(.05\ m)^2$, $\Delta x = t = 5x10^{-4}$ m. The required power is

for silicon: 406 watts at 25 °C, 56 watts at 700 °C;

for quartz: 27 watts at 25 °C, 33 watts at 700 °C.

Hence, for silicon substrates at high temperatures and quartz substrates at all temperatures, vertical thermal gradients within the substrate will have a significant effect on curvature unless the furnace used has a low vertical heat flux within the compartment holding the substrate.

Horizontal thermal gradients may also exist in the substrate. They induce thermal stresses that can alter the curvature of an

already-curved substrate, but the analysis of this effect will not be attempted here.

7. Summary

We have seen that the standard equation relating substrate curvature to film stress is theoretically accurate under certain experimental conditions and not accurate under others. Gravitational forces can cause a large error, but one can circumvent this problem by using small substrates or reproducible supports. The shape of the substrate, as long as it is a thin plate, does not affect the curvature-stress relation; neither does the crystallinity of (111)- or (100)-oriented cubic-material substrates. Thermal gradients can significantly alter substrate curvature. These pieces of information should be valuable to researchers measuring stresses in thin films on substrates.

References

1. G. G. Stoney, "The Tension of Metallic Films Deposited by Electrolysis," *Proc. Roy. Soc. (London),* vol. A82, p. 172,1909.

2. R. W. Hoffman, "The Mechanical Properties of Thin Condensed Films," in *Physics of Thin Films*, vol. 3, G. Hass and R. E. Thun, Eds. New York: Academic Press, 1966, p. 211.

3a. R. J. Roark, W. C. Young, *Formulas For Stress and Strain*, 5th ed. New York: McGraw-Hill, 1975, p. 405.

3b. Ibid., p. 324.

3c. Ibid., p. 583.

4. P. A. Flinn, D. S. Gardner, and W. D. Nix, "Measurement and Interpretation of Stress in Aluminum-Based Metallization as a Function of Thermal History," IEEE Trans. Elec. Dev., vol. ED-34, no. 3, pp. 689-699, 1987.

5. N. N. Davidenkov, "Measurement of Residual Stresses in Electrolytic Deposits," *Soviet Physics--Solid State*, vol. 2, pp. 2595-2598, 1961.

6. P. Townsend, D. M. Barnett, and T. A. Brunner, *J. Appl. Phys.*, in press.

7a. W. Flugge, Ed., *Handbook of Engineering Mechanics.* New York: McGraw-Hill, 1962, p. **39**-1.

7b. Ibid., p. **39**-26.

8. R. C. Weast, Ed., *CRC Handbook of Chemistry and Physics*, 59th ed. Boca Raton, Florida: CRC Press, 1979, p. F-80.

9. S. Timoshenko, *Strength of Materials, Part 2,* 3rd ed. Huntington, New York: Krieger, 1956, pp. 86-89.

10. W. A. Brantley, "Calculated Elastic Constants for Stress Problems Associated with Semiconductor Devices," *J. Appl. Phys.*, vol. 44, pp. 534-535, 1973.

11. Y. S. Touloukian, R. K. Kirby, R. E. Taylor, and P. D. Desai, Eds., *Thermal Expansion*, vol. 13. New York: IFI/Plenum, 1977.

12. Y. S. Touloukian, Ed., *Thermophysical Properties of High Temperature Solid Materials*, vol. 1 and vol. 4, part 2. New York: Macmillan, 1967.

B. Study of Metal Cracking in Interconnect Metals

(Anne I. Sauter)

1. Introduction

Aluminum metallization is commonly used as an interconnection material in integrated circuits. The continued functioning of such devices depends sensitively on the interconnect lines remaining continuous. Unfortunately, these lines are susceptible to cracking or void development as a result of several different types of conditions encountered in the fabrication and operation of integrated circuits, and if the lines crack or form voids, the device can fail. Causes of cracks or voids in lines can include electromigration, chemical reactions between the aluminum and an adjacent material, and high stresses developed in the lines as a result of the difference in thermal expansion coefficients between Al and silicon or silicon dioxide. The former two of these problems are fairly well understood and have been studied in a systematic way [1-3]. The last problem mentioned, however, which is known as the metal crack problem, although well known to engineers, is not understood in a fundamental way. There is no consensus as to the basic mechanisms of crack formation and growth due to thermal stresses.

The difficulty arises in this way. The deposition of Al is generally the second to last step in the fabrication of a device, the last step being the passivation layer depcsition. The passivation consists of an insulating material, usually silicon dioxide or silicon nitride, and this material is normally deposited at high temperatures (300-500°C). On cooling to room temperature, high stresses can develop in the Al lines due to the difference in thermal expansion coefficients, which is about 2.2 x 10-5 °K-1 between Al and Si. Since the lines are bonded on all sides to other materials (Si and SiO2), only a minimum of plastic flow can occur, if any at all, to relieve the stresses. Thus other mechanisms must come into play. It has been generally observed that cracks can form in the lines, presumably as a result of the high thermal stresses; what is not known is how these cracks initiate and grow. To discover how this cracking occurs is the object of this study.

2. Background

Some existing work by other authors provides a foundation for the present work. For example, the stresses due to thermal expansion differences in Al thin films on Si wafers have been studied via a wafer curvature method for various film thicknesses [4,5]. Mechanical properties of Al thin films such as hardness and yield strength have also been measured [6,7]. This information will be useful in the present study. In addition, several authors have addressed problems more closely related to the metal crack problem.

Jones used a finite element method to calculate stresses in Al lines on cooling after passivation deposition at 400°C [8]. He studied one micron thick Al-1%Si on oxidized Si passivated with 1.2 microns of PSG, in the form of lines of widths 1-6 microns. He found triaxial stress conditions conducive to the formation of creep voids. The smaller line widths resulted in higher stresses. This is consistent with intuition, and also with the observation that smaller lines have higher failure rates. The stresses he calculated in the line length direction for the 2 micron wide line are about the same (300-400 MPa) as those calculated previously by this author and reported in the progress report of March 1987.

Owada et al observed stress induced "slit-like" voids at grain boundaries in bamboo-type grain structures in passivated Al-Si patterned interconnections during aging tests at 200 °C [9]. The stresses driving the void formation were found to be a result of the presence of the passivation layer. They found that they could inhibit the appearance of the voids by preventing a bamboo-like grain stucture from forming, and concluded that a grain boundary migration mechanism was responsible for their formation. However, this does not seem to be a general solution to the metal crack problem, since their stress levels were relatively low because their tests were done above room temperature.

Both of these papers relate to the "metal crack problem," since in both cases voids in interconnections result from thermal stresses. The two authors arrive at different mechanisms to explain the void formation, however, and this

is typical of the confusion surrounding the problem. While is is quite possible that both of these mechanisms could operate in different regimes, it is not clear what these regimes are. A fundamental study is needed to accurately identify the mechanisms involved in interconnect crack formation, and the conditions under which each mechanism operates. Ultimately, it is hoped that methods will be developed to inhibit these mechanisms, so that crack formation can be prevented.

3. Metal Crack Problem Study

Test structures of Al-1%Si lines on oxidized Si passivated with sputtered SiO2 are being fabricated (Figure 1). These will be subjected to heating and cooling cycles in the wafer curvature apparatus, and stress information as a function of time and temperature will be obtained. If a sample is held at a temperature where a high tension stress exists in the lines, this stress will tend to relax. Since plastic flow of the lines is inhibited by the surrounding material, this relaxation will largely take the form of cracks in the lines. As the cracks form and the stress relaxes, the curvature of the wafer changes. The rate of change of the wafer curvature will yield stress relaxation data, from which can be calculated the rate of cracking and finally an activation energy for crack formation. This in turn will permit us to identify the mechanism of crack formation and growth. If there are different mechanisms that operate in different stress/temperature regimes, this will be made evident by calculating stress relaxation data for different temperatures.

Description of Samples

Single crystal double polished (100) Si wafers 4" in diameter and 500-550 microns thick were used. These were oxidized to form a 1000A layer of SiO2. Al-1%Si was sputter deposited to a thickness of 2 microns, patterned into lines and passivated with sputtered quartz.

Double polished wafers were used so that a smooth surface can be presented to the wafer curvature apparatus -- the side with the lines on it is bumpy, so the wafers are turned over to be measured. The thicknesses of the

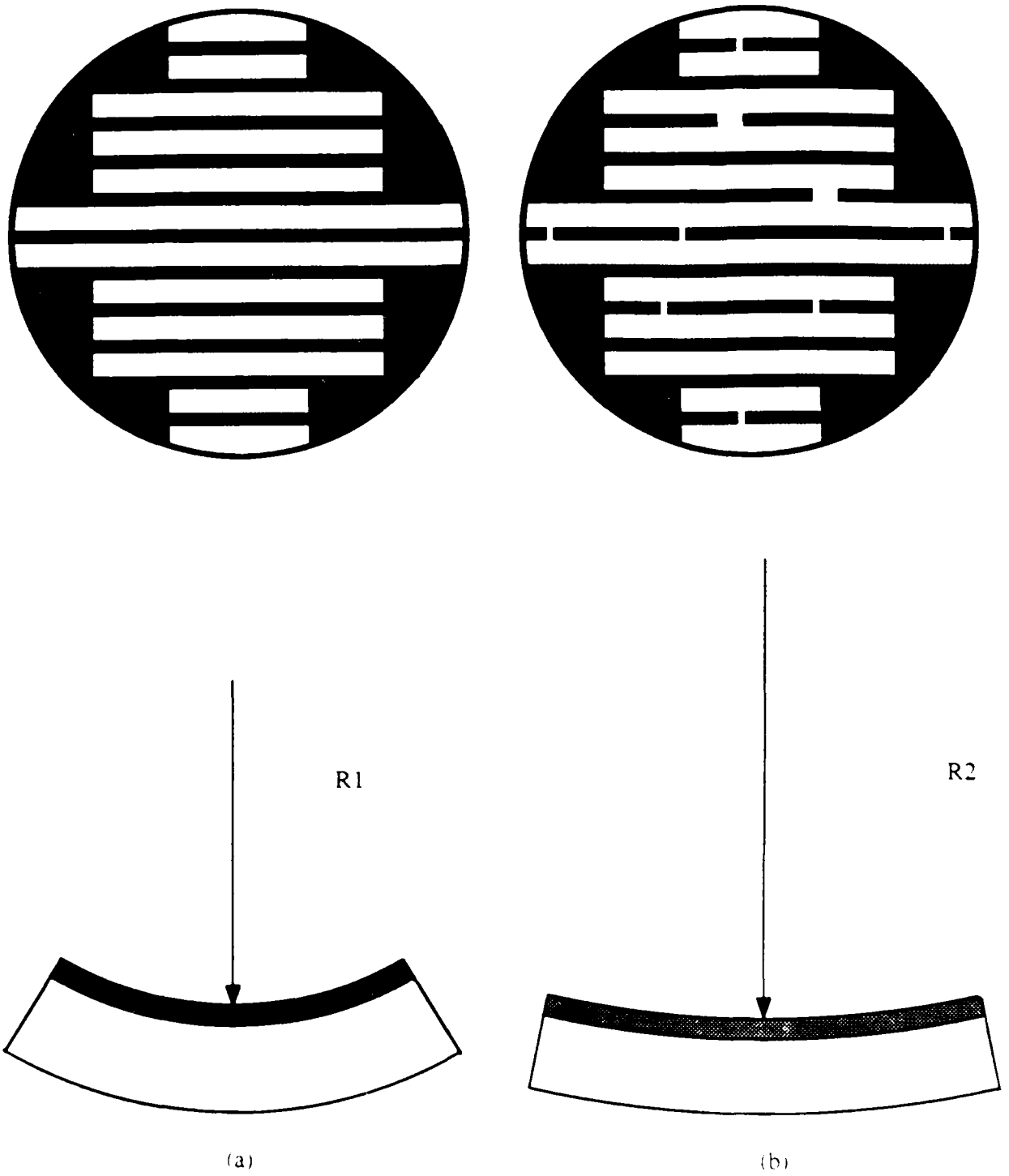

Figure 1: A schematic representation of the configuration of the samples. The lines are actually two microns wide and four microns apart. In (a), the lines are intact and the stresses in them have resulted in a curvature of radius R1. In (b), some of the lines have cracked, with the result that the stress has relaxed and the radius of curvature has changed to R2.

materials deposited were chosen to be representative of actual practice. Al-1%Si was used for the same reason. Sputtered quartz was chosen as a passivation material for several reasons. It is already to a large extent densified as it is deposited, so densification and outgassing of the passivation will not interfere with the stress measurements of the lines. In addition, sputtered quartz deposition is a room temperature process, which means that the lines are relatively stress free to begin with, and they can be stressed in a controlled fashion through temperature cycling. Although large initial tensile stresses in the lines require a high temperature deposition process, the sputtered quartz passivated samples will allow us to establish the stress/temperature characteristics of the lines independent of passivation stress effects. Later high temperature deposited passivations will be used to allow us to generate high tensile stresses in the lines and observe significant stress relaxation by cracking.

The pattern etched into the Al layer is basically a series of parallel lines. The lines are 2 microns wide, a typical dimension in practice. They are separated center to center by 6 microns, leaving 4 microns of bare oxide between each line. This should be sufficient to prevent significant interaction, that is, the lines should act like well separated lines and not a continuous layer of Al. The nature of the patterning machine is such that the whole wafer cannot be uniformly covered with lines, but there must be some patches near the edges that are either bare oxide or continuous Al. We chose to leave these covered with Al in order that the lines adjoining the patches be better anchored.

Description of Experiments

Since the passivation is deposited in a room temperature process, the samples should be relatively stress free at the outset, although there may be some low level of stress due to the fact that the sample is heated slightly during Al deposition. Significant cracking leading to stress relaxation will therefore probably not be observed in these samples, however as a first step this simple system can yield valuable information. It is also possible that some stress relaxation can be measured even at these low levels of stress.

The first measurements to be done would establish the stress/temperature dependence of the samples. Schematically, this might look like the analagous curve for thin film Al, with the lines going into compression on heating and tension on cooling. This information will assist in separating passivation stress effects from stresses in the lines when samples with high temperature deposited passivation layers are tested.

Samples will be fabricated identical to the samples described above but with a passivation layer deposited at a high temperature. This will enable high tensile stresses to be produced in the lines. Various stresses could then be imposed on the lines by holding at various temperatures at which the stresses are known through the first step. The amount the stress relaxes as a function of time is a measure of the amount of cracking in the lines. Obviously, the cracking is nonreversible, but hopefully there are enough lines on each sample that each could be used several times. The amount of cracking that occurs and the number of lines that crack depends on the initial stress level. If only a few percent of the lines must crack to produce a measurable curvature change, then many uncracked lines may remain after the experiment and the sample could possibly be used again.

4. Summary

A basic study of the mechanisms of metal crack formation in Al interconections is being undertaken. Test structures consisting of passivated Al lines on oxidized Si are being fabricated. These will be tested in the wafer curvature measurement machine to obtain stress relaxation data and ultimately information about the mechanisms of crack formation and growth.

References

1. G. DiGiacomo, IEEE Proc. Reliability Physics,19,218 (1981)
2. W.M. Paulson and R.P. Lorigan, IEEE Proc. Reliability Physics, 14,42 (1976)
3. C.F. Dunn, F.R. Brotzen and J.W. McPherson, J.Electr. Mat., 15,273 (1986)

4. P.A. Flinn, D.S. Gardner, and W.D. Nix, IEEE Trans. on Electron Dev.,34 (1987)
5. A.K. Sinha and T.T. Sheng, Thin Solid Films, 18,117 (1978)
6. M.F. Doerner and W.D. Nix, Interim Scientific Report,15 (1987)
7. E.M. Philofsky and K.V. Ravi, IEEE Proc. Reliability Physics, 11,33 (1973)
8. R.E. Jones, Jr., Preprint, IEEE Proc. Reliability Physics (1987)
9. N. Owada, K. Hinode, M. Horuchi, T. Nishida, K. Nakata, and K. Mukai, Preprint, published by IEEE (1985)

C. The Numerical Analysis of the Interaction of a Screw Dislocation with a Coherent Interface

(J. F. Turlo)

The interaction between dislocations and various obstacles dispersed throughout a crystalline material play a major role in the determination of the mechanical properties of the material. In a bulk material, the interaction of a dislocation with the surface is insignificant. However, in a thin film, the surface, or any interface, may become a prevalent obstacle to dislocation motion and, therefore, affect the mechanical behavior. So, an estimate of the force, or shear stress, required to pass a dislocation through an interface is important.

In 1953, Head examined the interaction of a screw dislocation with the interface between two materials of different shear modulus. In his treatment, the force of interaction becomes infinite at the interface. The common model of the dislocation views the dislocation as the line separating sheared from unsheared material with the line being a singularity yielding the infinite interaction stress. In 1969, Mura and Pacheco applied the Peierls model of a dislocation to the problem to obtain a finite interaction stress. In the Peierls model, the dislocation line, with Burgers' vector, b, is replaced by a continuous distribution of dislocation segments whose sum through the material is b. The total interaction stress is obtained by integrating the contribution from each infinitesimal dislocation segment over the whole material.

An external shear stress must be applied to the material to balance the force of the interface and prevent the dislocation from moving. The resulting equilibrium equation on the slip plane is

$$\int_{-\infty}^{-} \frac{1}{x-t}\frac{d\Psi}{dt}dt + \kappa \int_{-\infty}^{\bullet} \frac{1}{|x|-t}\frac{d\Psi}{dt}dt + \kappa \int_{\bullet}^{-} \frac{1}{|x|+t}\frac{d\Psi}{dt}dt + \frac{1}{2}\sin 2\pi\alpha = \frac{1}{2}\sin 2\pi\Psi \qquad (1)$$

where Ψ is the displacement of the atomic planes due to the dislocation and the applied shear stress, x is the spatial variable, α represents the applied shear stress and, κ is the relative shear modulus

$$\kappa = \frac{G_2 - G_1}{G_2 + G_1} . \qquad (2)$$

The first integral represents the shear stress on the slip plane from the dislocation alone and the next two integrals represent the shear stresses from image forces through the interface. The next term is the externally applied shear stress. The last term represents the resistance of the crystal to motion on the slip plane which is periodic as the crystal lattice. The equation is difficult to solve directly because of the singular integrand in the first integral as well as the nonlinearity of the sine terms.

If $\kappa = 0$ then the material is homogeneous, it has no interface. No force is required to hold the dislocation and the shape of the atomic planes is given by

$$\Psi_0 = \frac{1}{\pi} \arctan (x - c) \qquad (3)$$

where c is arbitrarily chosen as the center of the dislocation. This is the Peierls solution for the shape of a screw dislocation in an infinite material. As the infinite material is traversed from one end to the other, the shape function ranges from -0.5 to 0.5 which is one unit of shear, the Burgers' vector.

Mura and Pacheco added a correction function to the homogeneous solution to solve for the case including an interface. The even part of the correction function was expanded in a Taylor's series to obtain a first order solution, the odd part makes no contribution to first order. The infinite series obtained is somewhat unwieldy and provides no means of estimating the error of the solution, so some effort has been devoted to numerically obtaining a more complete solution.

The first attempt was to expand the displacement distribution as an asymptotic series,

$$\Psi = \sum_{n=1}^{\infty} \kappa^n \Psi_n . \qquad (4)$$

Since κ is always less than 1, the series will always converge if the Ψ_n are well behaved.

For n = 0, the homogeneous equation and solution are obtained. For n = 1, the equation for the first order correction is given as,

$$\int_{-\infty}^{-} \frac{1}{x-t}\frac{d\Psi_1}{dt}dt + \int_{-\infty}^{\bullet} \frac{1}{|x|-t}\frac{d\Psi_\bullet}{dt}dt + \int_{\bullet}^{-} \frac{1}{|x|+t}\frac{d\Psi_\bullet}{dt}dt + \pi\alpha_1 = \pi\Psi_1 \cos 2\pi\Psi_\bullet \quad (5)$$

A simple numerical quadrature formula was chosen and the results are shown in Figure 1.

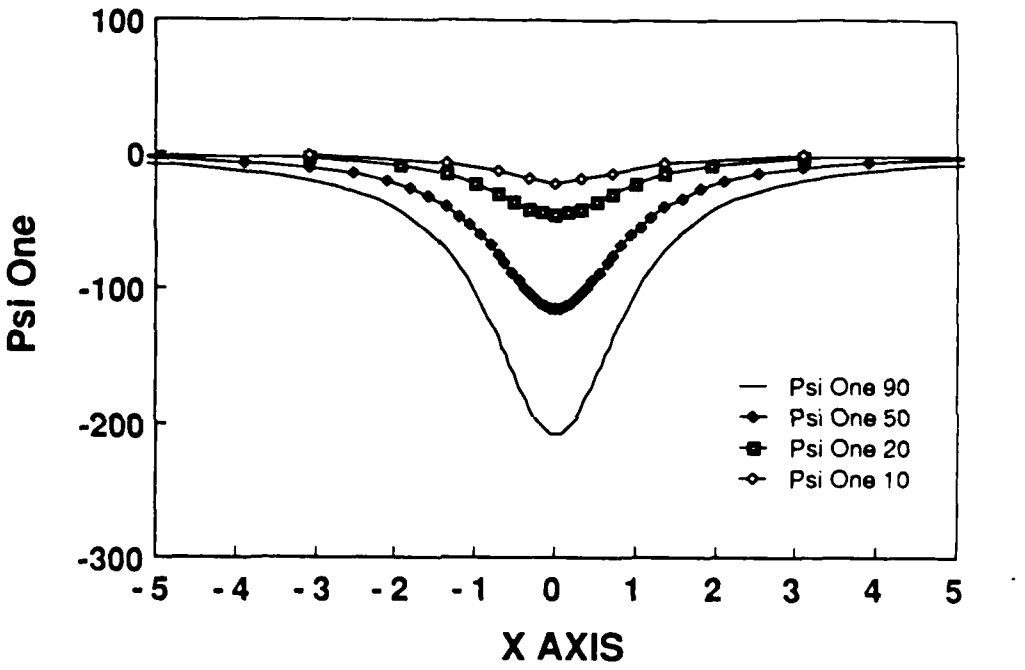

Figure 1. The first order correction to the homogeneous solution for the shape of a screw dislocation in the presence of an interface. The parameter is the number of points used to approximate the function Ψ_1.

As can be seen in the graph, Ψ_1 increases without bound at x = 0, as the number of points goes up, which implies a singularity in the solution. In fact, if the Peierls arctangent solution is substituted for Ψ_0 in equation (5), the integrals yield a logarithmic singularity at x = 0. So, the asymptotic expansion is not well behaved and, another approach must be developed.

Following Mura and Pacheco, the shape function can be represented as a first order solution plus a correction function,

$$\Psi(x) = \Psi_0(x) + D(x) \tag{6}$$

where Ψ_0 is the same as before and D is a lumped correction term. The resulting equation for D is,

$$\int_{-\infty}^{\infty} \frac{1}{x-t}\frac{dD}{dt}dt + K\int_{0}^{\infty}\frac{1}{|x|+t}\left[\frac{dD}{dt}(t) + \frac{dD}{dt}(-t)\right]dt - \frac{x-c}{1+(x-c)^2}\cos 2\pi D$$

$$-\frac{1-(x-c)^2}{2\left[1+(x-c)^2\right]}\sin 2\pi D = -\frac{1}{2}\sin 2\pi\alpha - \frac{x-c}{1+(x-c)^2} - \frac{K(|x|+c)\left[\frac{\pi}{2} + \arctan c\right]}{\pi\left[1+(|x|+c)^2\right]}$$

$$-\frac{K(|x|-c)\left[\frac{\pi}{2} - \arctan c\right]}{\pi\left[1+(|x|-c)^2\right]} + K\ln\left[\frac{|x|}{(1+c^2)^{\frac{1}{2}}}\right]\left[\frac{1}{\pi\left[1+(|x|+c)^2\right]} + \frac{1}{\pi\left[1+(|x|-c)^2\right]}\right] \tag{7}$$

which now includes both the sine and cosine functions. However, the magnitude of D is expected to be much less than one for small values of κ so, the equation can be linearized by the approximations that sinp = p and cosp = 1. The results of the numerical solution are shown in Figure 2. The graph exhibits the expected shape as well as an appropriate magnitude but, even this small magnitude is at the limit of the approximations made. Assuming the solution obtained at 89 points is close to the true solution, an approximate error can be obtained as a function of 1/N, the interval size, where N is the number of points. The behavior of the error for the quadrature method used can be predicted and is expected to behave as a power series in the interval size if the method is converging to the correct solution. Figure 3 shows a fourth order polynomial fit to the error showing that the quadrature method is converging appropriately.

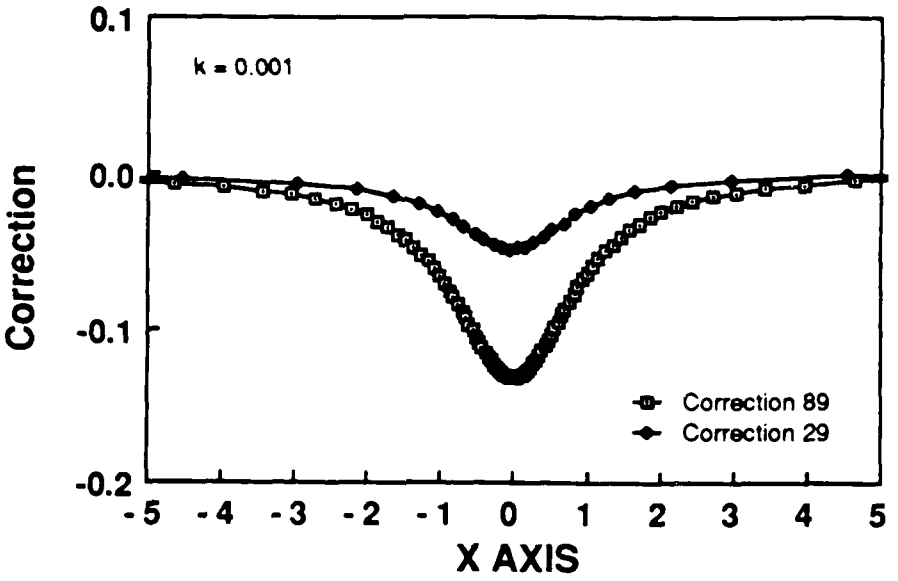

Figure 2. The first order approximation to the correction function, D. The parameter is the number of points used to approximate the function.

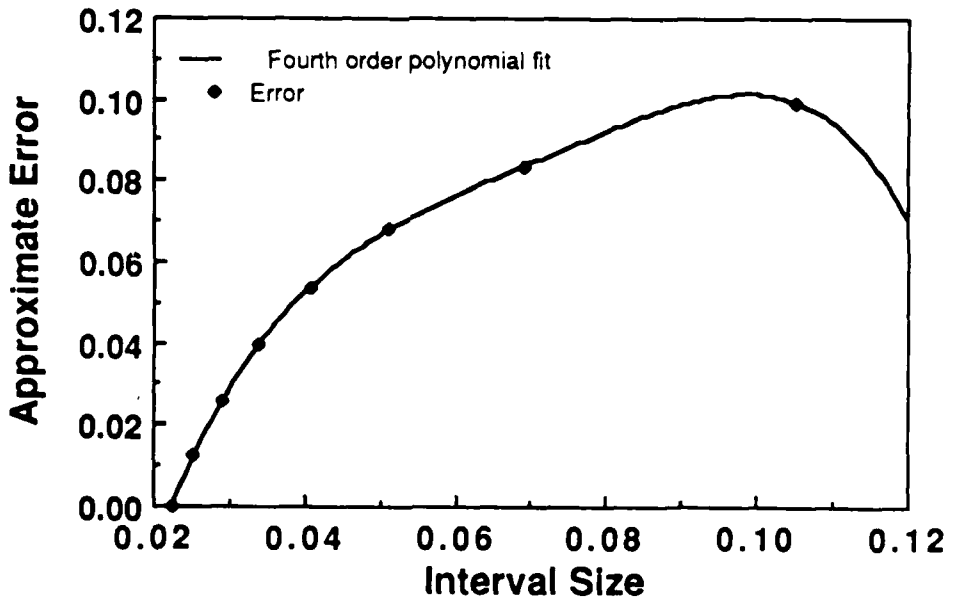

Figure 3. The approximate error as a function of interval size.

Figure 4 shows the result of adding the correction to Ψ_0 and Figure 5 shows the derivative of the approximate solution in Figure 4. Since the singular dislocation has been replaced by a continuous distribution of infinitesimal dislocations, the derivative of the shape function, Ψ, yields the magnitude of the dislocation through space. The derivative plot shows that the interface has forced the dislocation a small distance (approximately one fourth the Burgers' vector) into the softer material as expected from the attraction repulsion criterion established by Head.

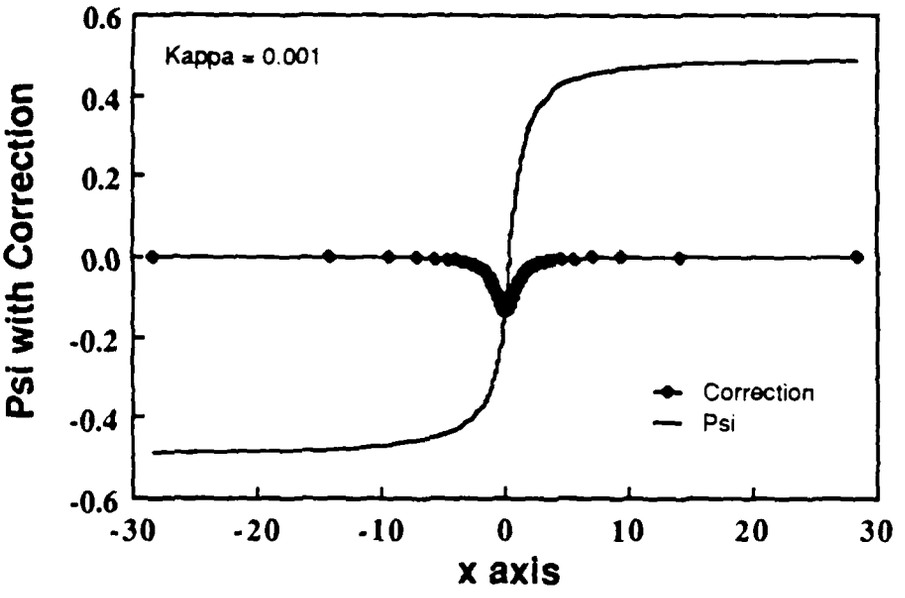

Figure 4. The shape distribution, Ψ, with the first order correction.

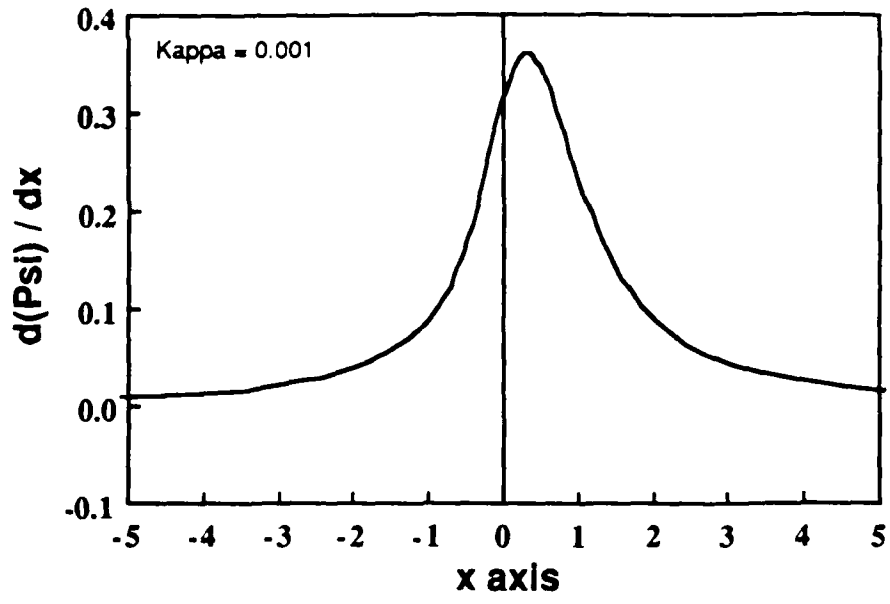

Figure 5. The derivative of the shape distribution.

The first order approximation of the stress required to hold the dislocation at any distance from the interface can be obtained and is given in Figure 6. Alpha is the shear stress normalized by the shear modulus. The maximum value occurs at the interface and represents the stress required to pass the dislocation through the interface or the theoretical strength of the interface. For an interface with a vacuum, $\kappa = 1$, the stress required to pass the interface is approximately one fifth the shear modulus.

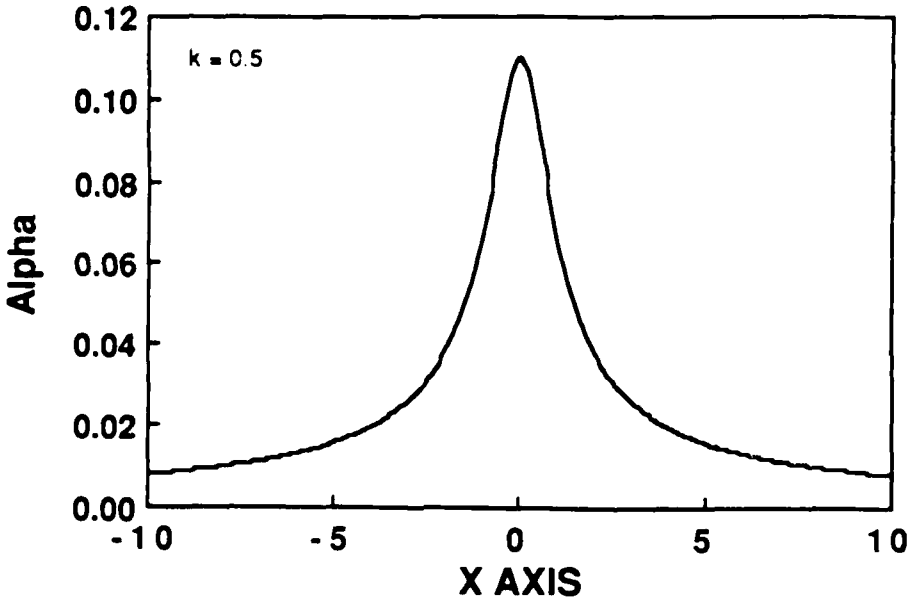

Figure 6. The first order approximation of the stress required to hold the dislocation in equilibrium.

The first order approximation is only accurate for very small κ so, the drastic approximations made to the sine and cosine functions must be improved. An attempt was made to add the next term in the sine and cosine series and solve iteratively but, the solution diverged. As a side note, an attempt was also made to solve equation (1) directly by applying a simple quadrature formula iteratively but, that also diverged. Several problems could be causing the failure including a programming error but, more likely is an inappropriate iterative technique or quadrature formula for this type of equation. More work is still necessary along the several lines still available.

III. Oral Presentations Resulting from AFOSR Grant No. 86-0051

1. W.D. Nix, "Mechanical Properties of Microelectronic Thin Film Materials", CIS Annual Review, Stanford University, March 6, 1986.

2. W.D. Nix, "New Experimental Techniques for the Study of Mechanical Properties of Microelectronic Thin Films", Department of Mechanical Engineering, University of California, Davis, March 13, 1986.

3. W.D. Nix, "Mechanical Properties of Thin Films and Other Fine Scale Structures", Albuquerque Chapter of ASM, Albuquerque, New Mexico, March 19, 1986.

4. M.F. Doerner, "Mechanical Properties of Thin Films Using Nanoindenter Techniques", Materials Science Industrial Affiliates Program, Stanford University, May 28, 1986.

5. M.F. Doerner and W.D. Nix, "Mechanical Properties of Thin Films on Substrates", Micromechanics Research Group, IBM Research Laboratory, San Jose, California, June 27, 1986.

6. W.D. Nix and M.F. Doerner, "Mechanical Properties of Microelectronic Thin Film Materials: Nanoindenter and Wafer Curvature Techniques", Summer Research Group, Materials Science Center, Los Alamos National Laboratory, August 18, 1986.

7. W.D. Nix, "Mechanical Properties of Thin Films", Materials Science Colloquium, Department of Materials Science and Engineering, Stanford University, December 5, 1986.

8. W.D. NIx, "New Experimental Techniques for the Study of Mechanical Properties of Thin Films", Department of Metallurgical Engineering, The Ohio State University, Columbus, Ohio, February 6, 1987.

9. W.D. Nix, "Mechanical Properties of Thin Films", Department of Materials Science, Ecole Polytechnique de Federale Lausanne, Lausanne, Switzerland, April 15, 1987.

10. M.F. Doerner, "Mechanical Properties of Thin Films using Sub-Micron Indentation Techniques", TMS Fall Meeting, Cincinnati, October 1987.

IV. Publications Resulting from AFOSR Grant No. 86-0051

1. M.F. Doerner and W.D. Nix, "A Method for Interpreting the Data from Depth-Sensing Indentation Instruments", J. Materials Research, 1, 601 (1986).

2. M.F. Doerner, D.S. Gardner and W.D. Nix, "Plastic Properties of Thin Fims on Substrates as Measured by Submicron Indentation Hardness and Substrate Curvature Techniques", J. Materials Research, 1, 845 (1986).

3. D.-B. Kao, J.P. McVittie, W.D. Nix and K.C. Saraswat, "Two-Dimensional Oxidation: Experiments and Theory", Proceedings of IEDM 85, IEEE, 1985, p. 388.

4. D.-B. Kao, J.P. McVittie, W.D. Nix and K.C. Saraswat, "Two-Dimensional Thermal Oxidation of Silicon: I. Experiments", IEEE Transactions on Electron Devices, ED-34, 1008 (1987).

5. P.A. Flinn, D.S. Gardner and W.D. Nix, "Measurement and Interpretation of Stress in Aluminum Based Metallization as a Function of Thermal History" IEEE Transactions on Electron Devices, ED-34, 689 (1987).

6. M.L. Ovecoglu, M.F. Doerner and W.D. Nix, "Elastic Interactions of Screw Dislocations in Thin Films on Substrates", Acta Metallurgica, 35, (1987).

7. D.-B. Kao, J.P. McVittie, W.D. Nix and K.C. Saraswat, "Two-Dimensional Thermal Oxidation of Silicon: II. Theory and Modeling", (accepted for publication in IEEE Transactions on Electron Devices).

8. M.F. Doerner and W.D. NIx, "Stresses and Deformation Processes in Thin Films on Substrates", (accepted for publication in Solid State and Materials Sciences).

9. M.F. Doerner and S. Brennan, "Strain Distribution in Thin Aluminum Films using X-ray Depth Profiling", (accepted for publication in Journal of Applied Physics).

END

DATE

FILMED

DTIC

4/88